VERIZONA PUBLISHER
Publishing Your Ideas

www.verizonaonlinepublishing.com
Vol: 1, Issue: 1

Journal of Electronics and Communication Engineering Research

A Self-consistent Method for Ring Artefact Correction in Tomographic Images

Davide Bianco

Italian Aerospace Research Centre, via Maiorise snc, 81043 Capua (CE), Italy

***Corresponding author:** Davide Bianco, Italian Aerospace Research Centre, via Maiorise snc, 81043 Capua (CE), Italy; E-mail: d.bianco@cira.it

Article Type: Research, **Submission Date**: 21 January 2016, **Accepted Date:** 16 February 2016, **Published Date:** 01 April 2016.

Citation: Davide Bianco (2016) A Self-consistent Method for Ring Artefact Correction in Tomographic Images. J. Elec. Commu. Eng. Resol 1(1): 1-5.

Abstract

A new, self-consistent method for the removal of ring-shaped artifacts in reconstructed tomographic images is presented, based on a different approach with respect to the currently adopted algorithms. Here, either afiltering of the sinogram or a modification of the final image could introduce further distortions. Starting from the difference between the original and a re-projected sinogram, our method is based on a dominant mode analysis similar to that originally introduced by Karhunen and Loeve. The algorithm has been tested numerically, and evidences of its accuracy are provided.

Keywords: Ring Artefacts, Tomography, Image Reconstruction.

Introduction

The use of micro-computed tomography (μ-CT) has gained considerable importance in the last three decades, since of its development in 1982 [1]. This wide success can be mainly ascribed to its large field of applicability. Exploiting the possibility of catching the details of structures at the scale length of micrometer, μ-CT has been used within many scientific frameworks, ranging from the bio-medical field to material science.

Scanners employed for μ-CT are composed of a fixed X-rays source, a fixed detectors' array, and a rotating sample. The uniform rotation around a given axis allows the acquisition of sample's projections at different angles. Beam attenuation is often measured using a two-dimensional high-resolution X-rays detector. This device consists in general of a scintillating material coupled with a photo-cathode and a charge coupled device (CCD) for digitalizing the data. It is particularly difficult to perform an accurate calibration of the entire apparatus. Using a fixed detectors' array, a miscalibration of a single device brings to a systematic error. The resulting bias in the corresponding attenuation leads to the introduction of ring-shaped artifacts in the reconstructed sample's cross-sections [2]. The use of a Filtered Back-Projection (FBP) [3,4] algorithm in the reconstruction enhances the effect of the offset. This is a result of the filtering procedure implicit in the method, which increases the relative strength of the high-frequency components.

Circular artifacts arising in reconstruction may also be due to the presence of dust on the surface of a detector, to a damage in one of the devices, a defective data acquisition system [5], or even being a consequence of the beam hardening effect [6].

Finally, ring-shaped structure in the reconstruction can be introduced by particular experimental configurations, in which, for instance, the time rays spent within the sample increases going from the edge to the centre. One example is a specimen with a square cross section projected at 45 degrees. The attenuation measured from the external detectors is systematically enhanced with respect to that measured in the centre. This results in ring-shaped artifacts, which can be easily confused with structural conformations of the specimen.

The removal of ring artifacts is important for enhancing the quality of μ-CT images, but can also be a crucial point for some applications. An example is the study of a displacement fields, to be retrieved from Digital Volume Correlation, DVC, exploiting the registration of two or more 3D tomographic images. Indeed, the underlying hypothesis is that the micro-structural features captured in the image are advected with the material itself. Artifacts that would be fixed with respect to the lab frame would clearly bias the displacement field measurement.

In literature, different methods have been proposed for removing ring-shaped artifacts. Available procedures can be cast into two sets. A first kind of approach consists of an *a-priori*analysis of the data. In this perspective, the measured attenuations are plotted within a sinogram, where the rows represent the different projection, and columns the responses of a single detectors at each angle. The biased data inducing the ring artifacts forms here brighter or darker vertical lines. Removing their offsets eliminates the ring-shaped structure in the reconstructed images.

Bias elimination can be performed in different ways. A first possibility is based on the fact that, in the Fourier transform of the sinogram, defective pixels form spikes at high frequencies. Their removal can then be obtained with a one dimensional Butterworth low pass-filter [7]. More recent works, employing a similar filtering procedure, try to enhance the performances of the filtering part, introducing sophisticated algorithms. In[8], spurious components are cut using a weighted median filter, similar to those employed for enhancing Signal-to-Noise ratio (S/N). In general, however, the filtering operations are detrimental to the resolution of images, and filtering parameters

are to be determined in a rather subjective fashion, making this class of procedures unsuited to metrological measurements [9].

Another method performs angular averages of the sinograms in order to highlight detectors' bias. The first step consists in summing the grey levels corresponding to one detector photosite, for all available projection. Smoothing out the average response provides an estimate of the detector's bias which is used to correct each single projection. One difficulty is that the average projection is theoretically expected to display a non smooth profile for sharp edged specimen. Thus the filtering is here again detrimental to the quality of the reconstruction as part of the signal is considered as noise [10]. Thus, in general the *a-priori* approaches are conceptually not completely satisfactory, since the partition between signal and noise cannot be decided on a general ground.

Another type of approach works *a-posteriori* on the reconstruction, as illustrated in [11]. Here, the image is analysed, in order to obtain a segmentation of the sample's section with respect to the background area. The Region of Interest (ROI) individuated in this way is processed to separate and eliminate the ring artifacts from the edge of the object. This kind of procedure often does not lead to a complete elimination of the artifacts, whereas some of the edges belonging to the object can be deleted.

In this work, we propose a new self-consistent method for the removal of ring artifacts, which can be ideally placed in between the two above mentioned approaches.

In fact, the algorithm relies on a transformation of the measured attenuations, as in the *a-priori*analysis. The difference is that the transformation of the sinogram depends on the first reconstructed image, resembling the*a-posteriori* approach.

The paper is organized as follows. Next section introduces the main underlying idea of the new method, together with some notation which will be used in the rest of the work. The third paragraph deals with the Karhunen-Loeve (KL) transform, which is used in the implementation of the algorithm. The fourth section presents a simple numerical application, together with a discussion of the results and some computational details. A paragraph summarizing conclusions and perspectives for the method ends the work.

Methods

Description

As recalled in the introduction, data acquisition in μ-CT involves a rotating specimen, a fixed X-ray source, and a fixed system for rays detection. In general, each radiograph $R(t,z,\theta)$ is indexed by θ, the angle between the fixed and the rotating frame, t, the radial coordinate, and z, which varies along the rotation axis of the specimen.

If the detector (vertical) axis and the rotation axis of the specimen are well aligned, constant z data will remain in the same detectors' plane under rotation. It is then convenient to consider the tomographic reconstruction as a two-dimensional problem, based on a sinogram $S(t,\theta)$, which for each z value is defined from the relation $S(t,\theta)=R(t,z,\theta)$. Reconstruction consists in computing the original absorption coefficient maps, $f(x)$, starting from the measured value of $S(t,\theta)$.

Performing a reconstruction is then equivalent to solving an inverse problem whose direct

$$\Pi_\theta \cdot f = S_\theta, \tag{1}$$

where f is a vector yielding the pixels decomposition of the sought reconstructed image $f(x,y)$, S_θ the vector containing the measured $S(t,\theta)$ sinogram, and Π_θ the projection matrix, with the parameter θ fulfilling the transformation equation

$$x\cos(\theta) + y\sin(\theta) = t, \tag{2}$$

between the fixed frame coordinates, x and y, and the rotated projection coordinate .

Even if the reconstruction problem, as formulated in Eq. 1, would be naturally tackled with an Algebraic Reconstruction Technique (ART) [12], the benchmark in this field is currently represented by the above mentioned FBP method [3,4].

Once that a solution, f, to the reconstruction problem has been found, it is straightforward to evaluate the action on it of the projection operator Π_θ. This yields a re-projected sinogram, S'_θ,which in an ideal situation should perfectly match S_θ. However, because of the imperfect signal acquisition, as well as of the inaccurate pixel representation, and other bias sources like the mis-alignment of detector and rotation axes, a non-zero residual $\Delta S = S' - S$.

The main idea is that this residual contains most of the biased response of the detector cell. In order to evaluate this biased component, the intensity recorded at a particular detector site, t_i, is assumed to be the true intensity scaled by a correction factor $1+\eta_i = 1+\eta(t_i)$, where the correction with respect to unity is assumed to be small, $\eta << 1$. Moreover, since the exposure time may fluctuate in between different radiographs, it has to be taken into account another scaling correction factor $1+\epsilon_i = 1+\epsilon(\theta_i)$, where it is again assumed $\epsilon<<1$.

The sinogram is constructed from the logarithm of the received intensity, scaled by the brightfield (assumed here to be uniform). Hence, with reference with the ideal sinogram, S_0 the measured one is

$$S(t,\theta) = S_0(t,\theta) + \eta(t)\,\epsilon(\theta). \tag{3}$$

The goal is to estimate both the one dimensional corrections, $\epsilon(\theta)$, and $\eta(t)$, starting from the two-dimensional residual ΔS. The following section describes the strategy which has been used.

Karhunen-Loevetransform

The issue to address is to determine a couple of functions, $\eta(t)$ and $\epsilon(\theta)$, whit a product equating the residual ΔS. This problem can be only formulated in a weak sense, since of the noisy character of ΔS and the larger amount of available measured data with respect to the unknowns.

For this reason, we chose to start from the minimization of the quadratic difference

$$T = \left(\frac{1}{2}\right)\iint \left(\Delta S(t,\theta)\right) + \eta(t)\,\epsilon(\theta)\Big)^2\, dt d\theta \tag{4}$$

Imposing null variations with respect to both η and ϵ leads to the system

$$\frac{\delta T}{\delta \eta} = -\int \left(\Delta S(t,\theta) - \eta(t)\,\epsilon(\theta)\right)\epsilon(\theta)\, d\theta = 0 \tag{5}$$

$$\frac{\delta T}{\delta \epsilon} = -\int \left(\Delta S(t,\theta) - \eta(t)\,\epsilon(\theta)\right)\eta(t)\, dt = 0$$

from which

$$\int \Delta S(t,\theta)\,\epsilon\,(\theta)\,d\theta = \eta\,(t)\int \epsilon\,(\theta)^2\,d\theta \tag{6}$$

and

$$\int \Delta S(t,\theta)\,\eta\,(t)\,dt = \epsilon\,(\theta)\int \eta\,(t)^2\,dt \tag{7}$$

Let us denote with $||\eta||$ and $||\epsilon||$ the $\mathcal{L}^2$ norm of η and ϵ respectively, and with $A = ||\eta||\,||\epsilon||$ their product. Combining the two equations above leads to

$$\frac{1}{A^2}\iint \Delta S(t,\theta)\;\Delta S(t',\theta)\,\eta\,(t')\;d\theta dt' = \eta\,(t), \tag{8}$$

and

$$\frac{1}{A^2}\iint \Delta S(t,\theta)\;\Delta S(t,\theta')\,\epsilon\,(\theta')\;d\theta' dt = \epsilon\,(\theta), \tag{9}$$

We can then introduce the two integral operators

$$\Phi\,(t,t')\,\underline{\underline{def}}\int \Delta S\;(t,\theta)\,\Delta S\,(t',\theta)\,d\theta, \tag{10}$$

and

$$\Psi\,(\theta,\theta')\,\underline{\underline{def}}\int \Delta S(t,\theta)\;\Delta S\,(t,\theta')\,dt, \tag{11}$$

using which the two equation to solve, Eqs. 8 and 9, take the form of two eigenvalue problems, namely

$$\int \Phi\,(t,t')\,\eta\,(t')\;dt' = A^2\,\eta\,(t), \tag{12}$$

and

$$\int \Psi\,(\theta,\theta')\,\epsilon\,(\theta')\;d\theta' = A^2\,\epsilon\,(\theta). \tag{13}$$

The solution to be retained is the one associated with the largest eigenvalue, $A^2 = \lambda$. The corresponding eigenvector η can be conventionally chosen to have a unit norm, $||\eta|| = 1$, so that $||\epsilon|| = \lambda^{1/2}$. It has to be noticed that it is unnecessary to solve both the eigenvalue problems, as they are related. Once that η has been determined, ϵ takes the form

$$\epsilon\,(\theta) = \int \Delta S\;(t,\theta)\,\eta\,(t)\,dt. \tag{14}$$

The procedure described here is similar to that proposed by Karhunen [13] and Loeve [14], usually dubbed KL-transform. In KL algorithm, all the terms coming from the diagonalization of either Φ or Ψ are retained. The main difference with our algorithm is that we need to retain only the dominants terms. This results in a significant enhancement of the computational effectiveness of the method.

Results and Discussions

A numerical test has been conducted on the new method, in order to assess its reliability and efficiency. Results show that the algorithm is fast, highly efficient, and easy to implement.

We start considering the sinogram generating the classical Shepp-Logan Phantom (SLP) [4], which for simplicity has been represented with a 512X512 pixels image. The attenuation are here modified in order to include, at some generic positions, an offset inducing ring-shaped structure in the reconstruction. The resulting sinogramis shown in Figure 1, where the offsets are represented as brighter horizontal lines. The bias has been randomly chosen between [0.1,0.2] of the mean value of the corresponding sinogram row.Despite the noteworthy offset

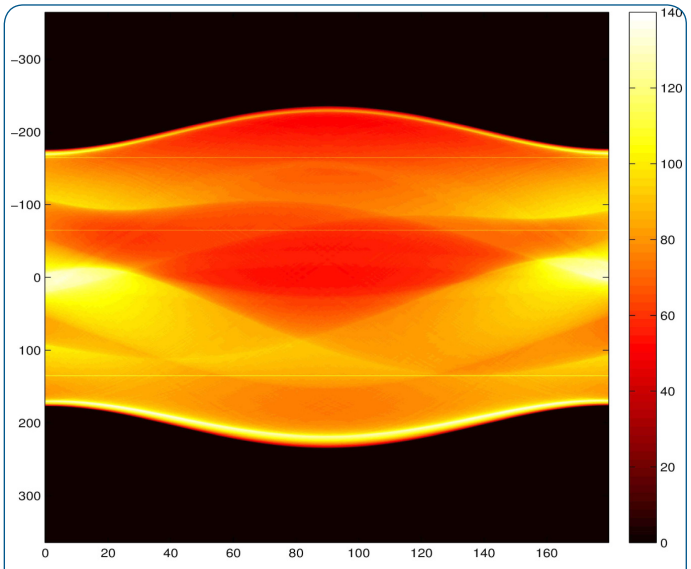

Figure 1: The original sinogram obtained with the re-projection of the Shepp and Logan Phantom has been modified in order to introduce ring-shaped artefacts within the reconstructed image

levels, the induced ring artefacts have been easily and accurately removed with the new self-consistent algorithm.

The modified attenuations, once filtered, are back-projected to reconstruct the SLP. The image is then re-projected itself, in order to obtain the sinogram S'(t,θ). In introducing the new algorithm, it has been argued that the biased detectors' response is mostly contained in the difference between S(t,θ) and S'(t,θ), namely ΔS. This initial ansatz is well verified, as shown in the upper panel of Figure 2, where the offsets can be identified as the brighter horizontal lines. The background, however, is neither uniform nor exactly zero. The proposed method has the advantage of avoiding the introduction of further noise, thanks to the exploitation of the dominant mode analysis.

As shown in the lower panel of Figure 2, the Karhunen-Loeve transform strongly enhance the ratio between the induced offset and the background. This achieved net separation allows a correct and automatic identification of the bias lines. The offset level so determined can be then subtracted from the original measured attenuation, and the SLP phantom reconstructed again. The difference between the corrected and the original SLP is shown in Figure 3. The comparison reveals the power of the method. As a matter of fact, the shown correction level has been reached with only one iteration. It can be observed that the reconstruction is nearly exact, as confirmed by the offsets value found a-posteriori

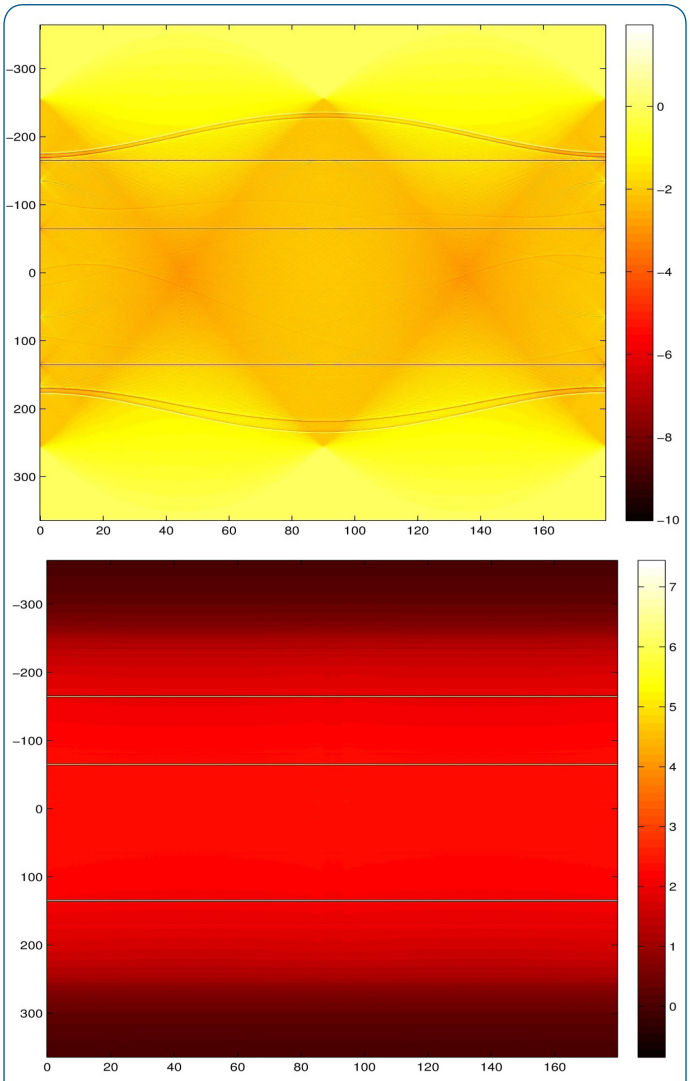

Figure 2: (up) The difference between the original and the re-projected sonogram clearly underlines the artefacts-inducing features of the measured attenuations. (down) The analysis carried on with the Karhunen-Loeve transform stresses the offset lines determining the ring shaped artefacts in the reconstructed image

with the KL method, as shown in Table 1. Moreover, working on the sinogram, the edges of the object are reproduced without smoothing or deletion effects.

Table 1: Offsets added to the phantom, in percentage, and the corresponding reconstructed values. The accuracy of the procedure is of the order of 1%

	1st line	2nd line	3rd line
added offset (%)	13.622	13.230	17.230
mean KL offset (%)	14.362	14.034	16.840

Conclusions and Perspectives

The new self-consistent method for the removal of ring artefacts in reconstructed tomographic image has shown to be powerful, in terms of accuracy, speed, and easiness of implementation. Moreover, it should in principle give more reliable results with respect to the currently adopted algorithms. As a matter of fact,

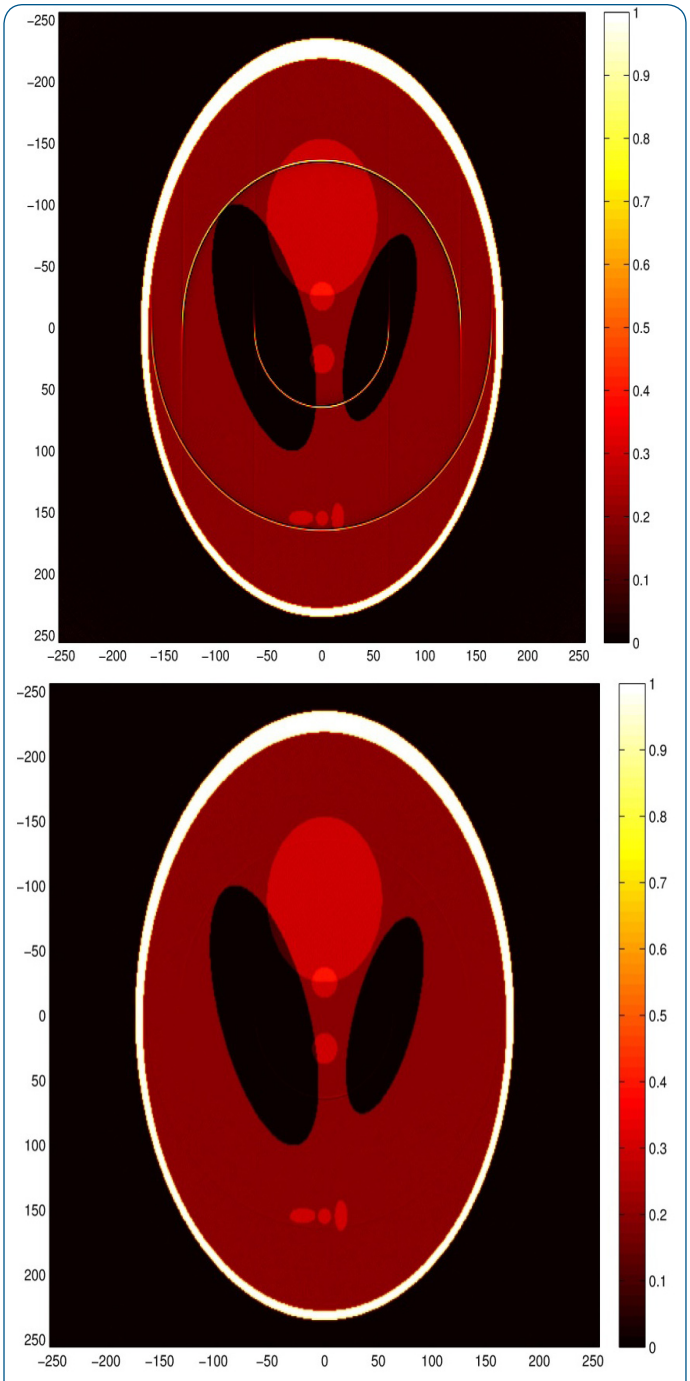

Figure 3: Comparison between the reconstructed Shepp and Logan Phantomsbefore (left) and after (right) the artefacts removal procedure

it is neither based on a filtering of measured attenuation, which could eliminate important data, nor on a modification of the final image, which could result in a distortion of the original reconstruction.

The removal of the artefacts is nearly exact, and gives the possibility of recon- structing an almost artefacts-free image. In perspective, a fine grain upgrading of the method will be investigated. The aim of this further research will be to lower of one order of magnitude the differences between the actual and the determined offsets, currently of the order of 1%.

References

1. Elliott JC, Dover SD. J. Microscopy. 1982; 126: 211.
2. Davis GR, Elliott JC. Nucl. Instr. Meth. Phys. Res. 1997; A394: 157.
3. Ramachandran GN, Lakshminarayanan AV. Proc. Nat. Acad. Sci. 1971; 68: 2236.
4. Shepp LA, Logan BF. IEEE Trans. Nucl. Sci. 1974; 21:228.
5. Munch B, Trtik P, Marone F, Stampanoni M. Optics Express. 2009; 17: 8567.
6. Munch B, Trtik P, Marone F, Stampanoni M. Comp. Geo. 2001; 27: 381.
7. Raven C. Rev. Scient. Instr. 1998; 69:2978.
8. Sadi F, Yeol Lee S, Kamrul Hasan Md. Comp. Bio. Med. 2010; 40:109.
9. Antoine C, Nygarda P, Gregersena OW, Holmstadb R, Weitkampc T, Rauc C. Nucl. Instr. Meth. Phys. Res. 2002; A490:392.
10. Boin M, Haibel A. Opt. Exp. 2006; 14:12071.
11. Sijbers J, Postnov A. Phys. Med. Biol. 2004; 49:N247.
12. Mueller K, Yagel R. IEEE Trans. Med. Imm. 2000; 19:1227.
13. Karhunen K. Ann. Acad. Sri. Fennicae. 1946; A1:37.
14. Loeve MM. Probability Theory. Van Nostrand:Princeton; 1955.